Influence of Spray Drying Parameters on the Formation of β-Phase Poly(vinylidene fluoride)

Jens Wiegmann[1,*], Sabine Beuermann[2], and Alfred P. Weber[1]

A simple one-step spraying method to produce poly(vinylidene fluoride) (PVDF) in the desired conformation is presented. The content of the piezoelectric β-phase is measured at different spray drying conditions and during electrospray. The influence of a strong electrical field and charges on the droplet are investigated separately from the electrospray setup with a pneumatic atomizer. For this purpose, the electric field is integrated into a pneumatic atomization process by a plate capacitor and the charge of the droplets by corona discharge. To investigate the drying properties, the drying temperature and the flow rate of dry air are examined. The presented process offers the possibility to deposit PVDF films or to produce PVDF powders, in their piezoelectric β- and γ-phases or in the nonpolar α-phase.

Keywords: Electrospray, Phase transitions, Piezoelectric β-phase, Poly(vinylidene fluoride), Spray drying

Received: August 31, 2020; *accepted:* April 20, 2021

1 Introduction

Besides common piezoelectric materials, also polymers can have piezoelectric properties. One representative is poly(vinylidene fluoride) (PVDF), which can be applied in sensor and/or actuator applications [1, 2]. With its high chemical and thermal stability, PVDF is a flexible and low-cost multifunctional material that can be used, e.g., for structural health monitoring applications in high-performance lightweight structures [3, 4]. PVDF occurs in five conformations. The crystalline β-phase of the polymer exhibits the strongest piezoelectric properties in comparison to the other four phases of the polymer [5]. The occurrence of the different phases depends on the production process and the treatment of the polymer. The transformation from the α-phase to the β-phase occurs, besides various possibilities, such as mechanical stress or the application of an electric field [6], through crystallization at low temperatures [7]. To form the desired piezoelectric active β-phase in a spray drying process, an important parameter is the evaporation rate and the crystallization rate of the dissolved PVDF droplets [7]. An aerosol process in which the PVDF particles can be prepared in a continuous one-step method by spray drying can avoid the common but expensive and batch-wise treatment. The evaporation rate is controlled by the amount of dry air given to the aerosol stream. A further investigated process parameter is the temperature, through which the evaporation rate can also be controlled. Within the scope of this project, it is investigated whether and under which process conditions the desired piezoelectric active β-phase or the γ-phase and α-phase are preferentially formed. The influence of the charge is considered in experiments with electrospray. Electrospray methods are used to produce thin piezoelectric polymer films [8, 9]. Some authors mention that the formation of the piezoelectric polar β-phase is favored by the presence of charge during the electrospray and the electrospinning process [9, 10]. Other publications show that positively and negatively charged nanofillers support the formation of β-phase PVDF [11, 12]. Further, it is suggested that solvated ions on the boundary layer between a solvent-containing PVDF and a precipitant phase during an anti-solvent process favor the formation of β-phase PVDF [13]. To investigate the phase transition process during electrospray in detail, the influence of the electric field and the charge on a droplet is examined during a conventional, pneumatic spray drying process. Since the synthesis of PVDF with electrospray leads to the desired high content of β-phase but the throughput is low, it is one objective of this study to identify the relevant electrospray features which need to be integrated into the better scalable pneumatic spray drying process for a phase transformation. The overall aim of this work is to develop a spray drying process in which the content of the different phases is adjustable and to maximize the desired piezoelectric β-phase.

[1]Jens Wiegmann, Prof. Dr. Alfred P. Weber
jens.wiegmann@tu-clausthal.de
Clausthal University of Technology, Institute of Particle Technology, Leibnizstraße 19, 38678 Clausthal-Zellerfeld, Germany.

[2]Prof. Dr. Sabine Beuermann
Clausthal University of Technology, Institute of Technical Chemistry, Arnold-Sommerfeld-Straße 4, 38678 Clausthal-Zellerfeld, Germany.

2 Experimental Section

A simple one-step spraying method to produce PVDF in the desired conformation is presented. The experimental setup aims at understanding the formation of the different conformations. Further details are given in Sect. 3.

2.1 Materials

PVDF was produced with iodine transfer emulsion polymerization. This process is described elsewhere [14]. The molecular weight of the used PVDF is $8800\,g\,mol^{-1}$. N,N-Dimethylformamide (DMF, $\geq 99.5\,\%$) from CarlRoth was used to dissolve PVDF. The properties of the used PVDF/DMF solutions are shown in Tab. 1.

Table 1. Properties of the sprayed PVDF/DMF solutions.

Property	Electrospray	Two-fluid nozzle
Mass fraction PVDF in DMF [wt %]	1	10
Surface tension [mN m^{-1}]	33.3	32.4
Density [g cm^{-3}]	0.955	0.992
Conductivity [µS cm^{-1}]	184.3	
Viscosity [mPa s]	1.8	5.2

2.2 Experimental Setup

Two different setups are used for the atomization of the PVDF/DMF solution. In the first setup, electrohydrodynamic atomization (EHDA, electrospray) is used for the atomization of the PVDF/DMF solution (Fig. 1a). The setup consists of a nozzle, a syringe pump (KD Scientific 100 CE), a high voltage source, and a collector plate. The nozzle has an inner diameter of 0.41 mm and an outer diameter of 0.72 mm (Nordson EFD). The high voltage was supplied by a power supply (Fug HCN 35-35000). It is an open setup so that heat and mass exchange with the environment can take place. To the nozzle of the electrospray setup, a voltage of 14.5 kV is applied. The collector plate is grounded and the distance between needle and plate is 5 cm. Consequently, the applied electric field is 290 kV m^{-1}. The mass fraction of PVDF in DMF is set to 1 % in this experiment to achieve good spraying conditions. The electrospray is operated in multi-jet mode, as the most stable spraying conditions prevail. The flow rate of the syringe pump is set to 0.3 mL h^{-1}.

In the second setup, an atomizer with a two-fluid nozzle from TOPAS (ATM 220) is used. The mass fraction of PVDF in DMF is 10 % and the solution is atomized with 1.5 bar. The flow rate of the generated aerosol is 83 L h^{-1} and the mass flow rate of droplets is 2.44 g h^{-1}. This setup mainly consists of the atomizer, a drying tube where the generated droplets are mixed with compressed air for the drying process, and a filter (Fig. 1b). The drying tube has a length of 20 cm and a diameter of 2.5 cm. The added drying air can be preheated. To investigate the influence of the electric field on the phase transformation, a plate capacitor is built around the drying tube. The distance between the two plates is 5 cm and the applied direct current (DC) voltage varies between 0 and 30 kV. The influence of the charge was investigated with corona discharge. Hence, a high voltage between –25 and 25 kV was applied to a needle in order to ionize the drying air. The unipolar ionized air was again mixed with the generated droplets. This leads to a drying process and simultaneously to the charging of the droplets. The mass loading during the spray drying process was determined gravimetrically (Eq. (1)). The mass loading is determined by the ratio of the added precursor to the air supplied to the entire system. The mass loading is used to compare the electrospray setup with the pneumatic setup and to make the observations more general.

$$\text{Mass loading} = \frac{\text{Atomized solvent}}{\text{Atomization air} + \text{Drying air}} \qquad (1)$$
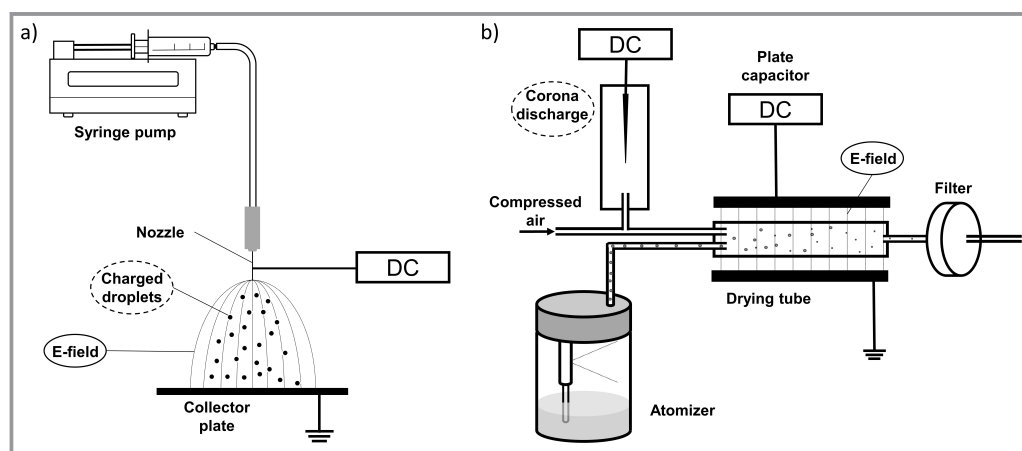

Figure 1. Experimental setup for the atomization with electrospray (a) and with a two-fluid nozzle (b).

2.3 PVDF/Particle Characterization

The phase analysis of the PVDF was conducted via Fourier transform infrared (FTIR) spectroscopy measurement with a Tensor 27 instrument from Bruker. The content of the α-, β-, and γ-phases is determined by analysis according to Gregorio et al. [15] (Eq. (2)) and Cai et al. [16] (Eqs. (3) and (4)).

$$F_{EA} = \frac{A_\beta}{1.3A_\alpha + A_\beta} \tag{2}$$

$$F(\beta) = F_{EA} \frac{\Delta H_{\beta'}}{\Delta H_{\beta'} + \Delta H_{\gamma'}} \tag{3}$$

$$F(\gamma) = F_{EA} \frac{\Delta H_{\gamma'}}{\Delta H_{\beta'} + \Delta H_{\gamma'}} \tag{4}$$

where F_{EA} is the electroactive β- and γ-content, A_β and A_α are the absorbance at 840 and 766 cm^{-1}, respectively. $\Delta H_{\beta'}$ and ΔH_γ are the absorbance differences between 1275 and 1260 cm^{-1} and between 1234 and 1225 cm^{-1}, respectively.

The particle size distribution was measured with an electrical low-pressure impactor (ELPI+ from DEKATI). The charge on the particles was measured with a Faraday cup electrometer (FCE). For this purpose, the filter was substituted with the FCE or the ELPI+ in the pneumatic setup. For the calculation of the charge per particle, the size of the particle determined by ELPI+ is used and the current signal obtained in FCE.

3 Results and Discussion

In the experiments with electrospray, PVDF/DMF droplets are produced. The generated droplets are charged and travel along the electric field to the grounded plate. On the way to the plate, the droplets dry completely, so that pure PVDF particles are deposited on the collector plate. Both parameters, i.e., charge and electric field, are present during the evaporation of the solvent DMF and, therefore, also during the formation of β-phase PVDF. The produced PVDF does not contain γ-phase and nearly no α-phase. The β-phase accounts for 90 % and the α-phase for 10 %. The FTIR spectrum of the electrosprayed PVDF is compared to an FTIR spectrum of a pneumatic two-fluid nozzle-sprayed PVDF at high mass loading conditions in Fig. 2. The β-phase peak at 1275 cm^{-1} is increased and the γ-phase peak at 1234 cm^{-1} is not present for PVDF from the electrospray setup. The α-phase peak at 766 cm^{-1} remains unchanged small. In the drying process during electrospray, the mass loading is 11 mg L$_{air}$$^{-1}$ and was estimated for a comparison between pneumatic spray drying and electrospray (Fig. 2). An advantage of producing a PVDF film by electrospray is that the produced β-phase is polarized in the applied electric field [9]. This means that a piezoelectric material is pro-
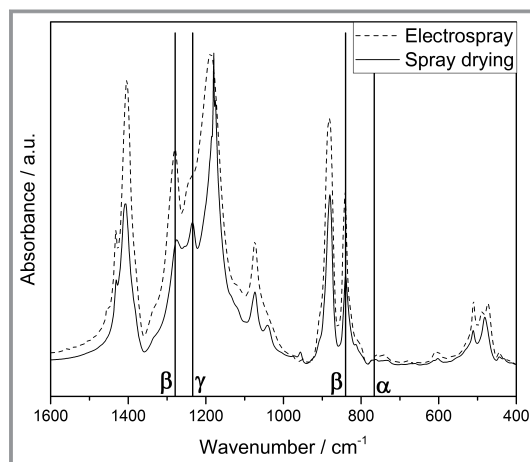

Figure 2. FTIR spectra of electrosprayed and pneumatic sprayed PVDF.

duced directly, which does not require any subsequent treatment.

The size distribution for dried PVDF particles from the second setup using a two-fluid nozzle atomizer is shown in Fig. 3. The particles have a size from 0.03 up to 5 µm and an x_{50} value of 102 nm. The size measurement was conducted at ambient temperature, a mass fraction of 10 % PVDF, and the mass loading of the solution was 15 mg L$_{air}$$^{-1}$.
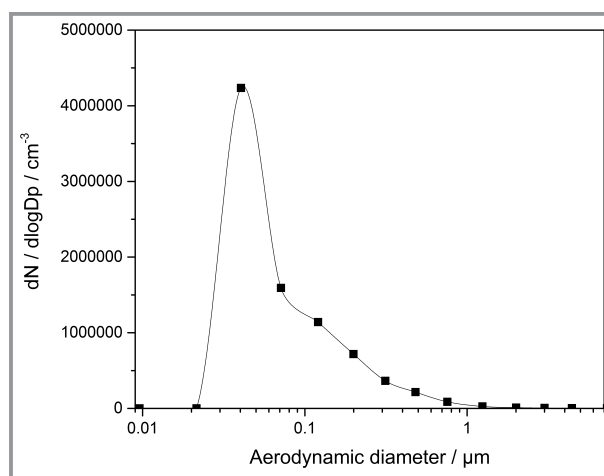

Figure 3. Size distribution of dried PVDF particles for atomization with a two-fluid nozzle.

Fig. 4 shows that the content of the α-, β-, and γ-phases changes when drying conditions are varied. The dry air is added with ambient temperature. At a mass loading of 15 mg L$_{air}$$^{-1}$, the mixture of aerosol to dry air is 1:1. The amount of dry air is increased up to a mixture of 1:5 and a resulting mass loading of 5 mg L$_{air}$$^{-1}$. The content of the β-phase increases, while the γ-phase decreases with a reduction of the mass loading. The content of the α-phase remains constant between 3.5 and 7 % for all mass loadings. At a mass loading around 5 mg L$_{air}$$^{-1}$, which means that the

mixture of aerosol to dry air is 1:5, the content of the γ-phase is near 0 %, and the β- phase reaches a constant value of around 95 %. High dry airflow rates reduce the time in which a drop evaporates completely and, therefore, increase the evaporation rate [17, 18]. The results indicate that a fast drying kinetic during spray drying favors the formation of β-phase PVDF. This can be explained with the Ostwald step rule. The Ostwald step rule states that first, in a reaction with several products, not the most stable form is reached, but rather the form closest to the free energy of the original state [19]. The α-phase is the most stable form followed by the γ-phase. The β-phase has the highest energetic state and, therefore, forms the most unstable crystal form [20]. Under the assumption of the Ostwald step rule, the β-phase is formed at fast evaporation kinetics. The formation of the γ-phase takes place at reduced evaporation kinetics and thus at increased mass loadings. Similar observations are made in the production of β-phase PVDF by a RESS (rapid expansion of supercritical solutions) process, in which nucleation also occurs fast [21]. Other publications show different results. It is mentioned that a high evaporation rate favors the formation of α-phase and reduces the formation of β-phase [7, 22]. In these studies, the evaporation rate is increased by an increase in temperature. In contrast to these studies, however, the evaporation kinetics in this spray drying process is influenced by the amount of drying air. Nevertheless, a similar behavior like in [7, 22] is observed for spray drying with preheated drying air (Fig. 5). The experiments were conducted with a high mass loading at $20.2\,\mathrm{mg\,L_{air}^{-1}}$ so that at 21 °C mostly γ-phase and no β-phase is produced. With increasing the temperature, the amount of γ-phase decreases while the amount of α- and β-phases increases. There are two effects of phase transformation. A higher temperature of the drying air enlarges the vapor pressure of the DMF and, therefore, the droplet evaporates faster [23]. The increase of the β-phase is caused by this increase of the evaporation rate, induced by higher temperatures, like the results shown in Fig. 4. The increase of the α-phase can be explained by the presence of higher temperatures like it is observed in [7, 22].

The spray drying with electrospray PVDF showed a high β-phase content compared to pneumatic spray drying with a similar mass loading (Fig. 4). This indicates that either the electric field or the charge on the droplets lead to an increased formation of the β-phase. In further experiments with the pneumatic two-fluid nozzle, an electric field and a corona discharger are added. The influence of the charge prevailing in electrospray and the electric field should be considered separately. The strength of the electric field during the electrospray is at $290\,\mathrm{kV\,m^{-1}}$. Strong electric fields can cause a change in the conformation towards the β-phase [24]. It was observed that electric fields of 100 MV m^{-1} lead to an enhanced formation of β-phase PVDF [20, 25]. During electrospinning, it is assumed that the polymer chains orientate towards the electric field and, therefore, the formation of the β-phase is favored [26, 27]. The
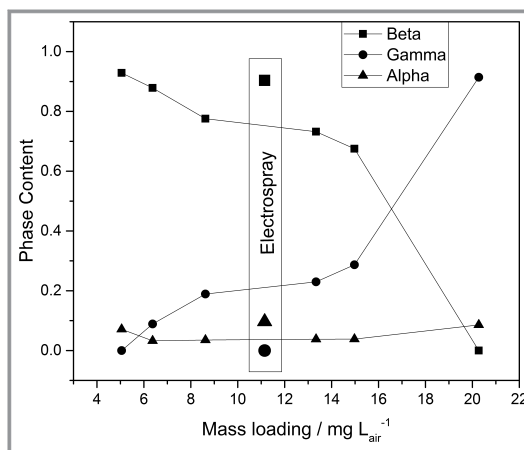

Figure 4. Crystalline phase conformations of the PVDF after spray drying at different mass loadings.
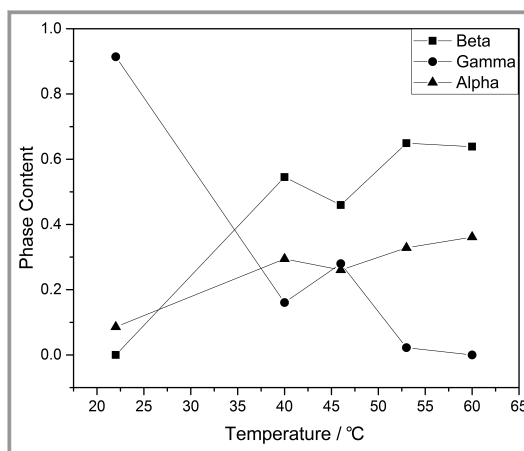

Figure 5. Crystalline phase conformations of the PVDF after spray drying at different temperatures.

increased mobility of PVDF molecules in the dissolved state could lead to an increased formation of the β-phase even in comparatively weaker electric fields. It is to be examined whether the comparatively weak electric fields of electrospray can lead to a phase transformation. The mass loading is set to $15\,\mathrm{mg\,L_{air}^{-1}}$. As can be seen in Fig. 6, there is no change in the phase composition with increasing electric field strength. The β-phase content remains constant even for strong electric fields at $600\,\mathrm{kV\,m^{-1}}$, which is more than twice as much as with electrospray. The electric field does not seem to be strong enough to induce interactions with the PVDF molecules.

However, there are indications that the presence of charge favors the formation of β-phase PVDF [9–13]. The influence of charge on the phase conversion during spray drying is tested with corona discharge. Fig. 7 shows the phase content in dependence of the applied voltage to the needle in the corona discharger, which is an indicator for the concentration of the produced ions. The highest amount of β-phase PVDF is achieved for a positive voltage of 25 kV at
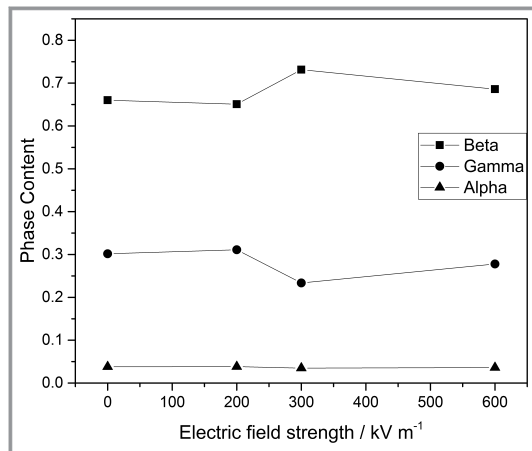
Figure 6. Crystalline phase conformations of the PVDF after spray drying in an electric field.

Figure 8. Charges per particle at different applied voltages in the charged spray drying process.

the needle. The phase content of β-phase PVDF decreases with the reduction of the voltage. When a negative voltage is applied, the content of β-phase PVDF reaches its minimum for –15 kV. When a higher negative voltage (–25 kV) is used, the β-phase content increases again but it is still below the β-phase content of 25 kV. The charge per particle (Fig. 8) indicates that the charging process for positive corona discharge is more effective. Without corona discharge, there are 20 negative charges per particle. The phenomenon that droplets originating from pneumatic atomization carry negative charge is known [28]. If the voltage is increased to 25 kV, there is a change from 20 negative charges to 57 positive charges per particle. But at a voltage of –25 kV, the charge only changes from 20 to 57 negative charges per particle. Taking into account the strength of charge change for the positive corona discharge, the increased β-phase formation can be explained for the positive corona discharge. Furthermore, a steric hindrance could reduce the formation of β-phase PVDF for negatively charged droplets. The covalent
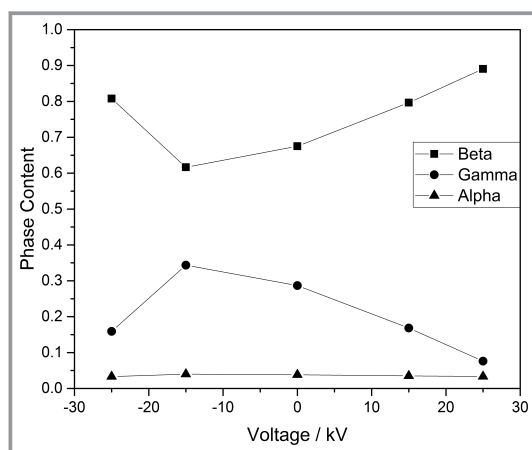
atom radius of fluorine (57 pm) is almost twice as large as that of hydrogen (31 pm) [29].

A schematical illustration of the phase conversion process during spray drying with charged particles is shown in Fig. 9. The charge applied to the droplet through corona discharge will distribute over the droplet surface due to repulsive forces. The dissolved PVDF molecules in droplets have a partial positive charge in the CH_2 segments and a partial negative charge in the CF_2 segments. When a positive voltage is applied to the corona discharger, the drop surface is positively charged and the partial positive CF_2 segments of the dissolved PVDF align themselves in the direction of the surface. The solvent of the drop evaporates, which leads to a reduction of the surface and simultaneously increases the charge density on the drop and the effect is enhanced. If the solvent evaporates sufficiently, crystallization occurs in the β-phase in the charge-forced arrangement. If a negative charge is applied, the arrangement of the PVDF molecule is reversed and CH_2 segments align themselves towards the droplet surface. The stronger curvature on the inner side of the molecule leaves less space for the larger fluorine atoms and, thus, causes steric hindrance in the formation of the β-phase. This could also explain why an increase in β-phase is observed for an applied voltage of +15 kV, but a slight decrease in β-phase at –15 kV. Stronger negative charges on the surface, as at 25 kV, however, lead to the effect shown in Fig. 9.

4   Conclusion

The spray drying process with the two-fluid nozzle enables the production of PVDF in the α-, β-, and γ-phases in different compositions. Each of the three phases can be adjusted through the variety of different spray drying and process parameters. By raising the temperature, the α-phase content can be increased. The piezoelectric β-phase can be produced by increasing the addition of drying air and

Figure 7. Crystalline phase conformations of the PVDF after spray drying with corona discharge.
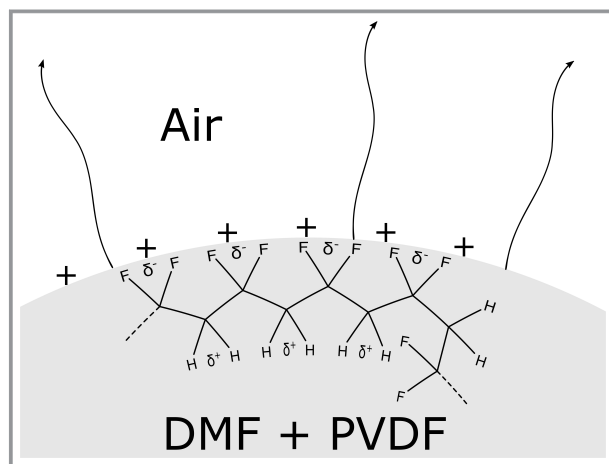
Figure 9. Schematic illustration of the β-phase formation in the charged spray drying process.

charging the drop surface during the drying process. The γ-phase is formed by a reduction of the drying air and, thus, by reduced drying kinetics.

Furthermore, this study shows that spray drying by means of electrospray has a positive influence on the formation of the β-phase. This is caused by the application of surface charge during the atomization process. The positive charge has a stronger influence on the formation of the β-phase than the negative charge. This could be explained by a steric hindrance by the fluorine atoms, which are almost twice as large as the hydrogen atoms. In general, the presence of charge on the droplet has a greater influence on the formation of the β-phase in contrast to an externally applied electric field where no influence on the formation of the phases could be observed. The positive influence of the charge on the formation of the β-phase can also be used in pneumatic spray drying by charging the droplets through corona discharge. Based on these results, charging processes directly at the two-fluid nozzle, e.g., by applying a voltage, could provide a more effective way of charging the droplets and, thus, enable high throughputs in pneumatic spray drying.

Symbols used

A_α	[–]	absorption at 766 cm^{-1}
A_β	[–]	absorption at 840 cm^{-1}
F_{EA}	[–]	electroactive β- and γ-content in PVDF
$\Delta H_{\beta'}$	[–]	absorbance differences between 1275 and 1260 cm^{-1}
$\Delta H_{\gamma'}$	[–]	absorbance differences between 1234 and 1225 cm^{-1}

Abbreviations

DC	direct current
EHDA	electrohydrodynamic atomization
ELPI	electrical low-pressure impactor
FCE	Faraday cup electrometer
FTIR	Fourier transform infrared
PVDF	poly(vinylidene fluoride)
RESS	rapid expansion of supercritical solutions

References

[1]   Y. Bar-Cohen, Q. Zhang, *MRS Bull.* **2008**, *33 (3)*, 173–181. DOI: https://doi.org/10.1557/mrs2008.42

[2]   P. Ueberschlag, *Sens. Rev.* **2001**, *21 (2)*, 118–126. DOI: https://doi.org/10.1108/02602280110388315

[3]   V. T. Rathod, D. R. Mahapatra, A. Jain, A. Gayathri, *Sens. Actuators, A* **2010**, *163 (1)*, 164–171. DOI: https://doi.org/10.1016/j.sna.2010.08.017

[4]   H. Gu, Y. Zhao, M. L. Wang, *Struct. Control Health Monit.* **2005**, *12 (3–4)*, 329–343. DOI: https://doi.org/10.1002/stc.61

[5]   P. Martins, A. C. Lopes, S. Lanceros-Mendez, *Prog. Polym. Sci.* **2014**, *39 (4)*, 683–706. DOI: https://doi.org/10.1016/j.progpolymsci.2013.07.006

[6] C. Ribeiro, V. Sencadas, J. L. G. Ribelles, S. Lanceros-Méndez, *Soft Mater.* **2010**, *8 (3)*, 274–287. DOI: https://doi.org/10.1080/1539445X.2010.495630

[7] R. Gregorio, D. S. Borges, *Polymer* **2008**, *49 (18)*, 4009–4016. DOI: https://doi.org/10.1016/j.polymer.2008.07.010

[8] J. Sakata, M. Mochizuki, *Thin Solid Films* **1991**, *195 (1–2)*, 175–184. DOI: https://doi.org/10.1016/0040-6090(91)90269-4

[9] I. B. Rietveld, K. Kobayashi, T. Honjo, K. Ishida, H. Yamada, K. Matsushige, *J. Mater. Chem.* **2010**, *20 (38)*, 8272. DOI: https://doi.org/10.1039/c0jm01265c

[10] F. Mokhtari, M. Latifi, M. Shamshirsaz, *J. Text. Inst.* **2016**, *107 (8)*, 1037–1055. DOI: https://doi.org/10.1080/00405000.2015.1083300

[11] Y. Wu, S. L. Hsu, C. Honeker, D. J. Bravet, D. S. Williams, *J. Phys. Chem. B* **2012**, *116 (24)*, 7379–7388. DOI: https://doi.org/10.1021/jp3043494

[12] M. S. Sebastian, A. Larrea, R. Gonçalves, T. Alejo, J. L. Vilas, V. Sebastian, P. Martins, S. Lanceros-Mendez, *RSC Adv.* **2016**, *6 (114)*, 113007–113015. DOI: https://doi.org/10.1039/c6ra24356h

[13] F. Lederle, C. Härter, S. Beuermann, *J. Fluorine Chem.* **2020**, *234*, 109522. DOI: https://doi.org/10.1016/j.jfluchem.2020.109522

[14] F. Brandl, S. Beuermann, *Chem. Ing. Tech.* **2018**, *90 (3)*, 372–379. DOI: https://doi.org/10.1002/cite.201700089

[15] J. R. Gregorio, M. Cestari, *J. Polym. Sci., Part B: Polym. Phys.* **1994**, *32 (5)*, 859–870. DOI: https://doi.org/10.1002/polb.1994.090320509

[16] X. Cai, T. Lei, D. Sun, L. Lin, *RSC Adv.* **2017**, *7 (25)*, 15382–15389. DOI: https://doi.org/10.1039/c7ra01267e

[17] I. Zbicinski, *Chem. Eng. J.* **2002**, *86 (1–2)*, 207–216. DOI: https://doi.org/10.1016/S1385-8947(01)00291-1

[18] I. Zbicinski, C. Strumillo, A. Delag, *Drying Technol.* **2002**, *20 (9)*, 1751–1768. DOI: https://doi.org/10.1081/DRT-120015412

[19] R. A. van Santen, *J. Phys. Chem.* **1984**, *88 (24)*, 5768–5769. DOI: https://doi.org/10.1021/j150668a002

[20] H. Su, A. Strachan, W. A. Goddard III, *Phys. Rev. B* **2004**, *70 (6)*, 064101. DOI: https://doi.org/10.1103/PhysRevB.70.064101

[21] S. Wolff, F. Jirasek, S. Beuermann, M. Türk, *RSC Adv.* **2015**, *5 (82)*, 66644–66649. DOI: https://doi.org/10.1039/c5ra12142f

[22] D. M. Dhevi, A. A. Prabu, K. J. Kim, *J. Mater. Sci.* **2016**, *51 (7)*, 3619–3627. DOI: https://doi.org/10.1007/s10853-015-9685-6

[23] F. K. A. Gregson, M. Ordoubadi, R. E. H. Miles, A. E. Haddrell, D. Barona, D. Lewis, T. Church, R. Vehring, J. P. Reid, *Phys. Chem. Chem. Phys.* **2019**, *21 (19)*, 9709–9719. DOI: https://doi.org/10.1039/c9cp01158g

[24] G. T. Davis, J. E. McKinney, M. G. Broadhurst, S. C. Roth, *J. Appl. Phys.* **1978**, *49 (10)*, 4998–5002. DOI: https://doi.org/10.1063/1.324446

[25] V. Sencadas, R. Gregorio, S. Lanceros-Méndez, *J. Macromol. Sci., Part B: Phys.* **2009**, *48 (3)*, 514–525. DOI: https://doi.org/10.1080/00222340902837527

[26] D. Dhakras, V. Borkar, S. Ogale, J. Jog, *Nanoscale* **2012**, *4 (3)*, 752–756. DOI: https://doi.org/10.1039/c2nr11841f

[27] J. Zheng, A. He, J. Li, C. C. Han, *Macromol. Rapid Commun.* **2007**, *28 (22)*, 2159–2162. DOI: https://doi.org/10.1002/marc.200700544

[28] M. Murtomaa, M. Savolainen, L. Christiansen, J. Rantanen, E. Laine, J. Yliruusi, *J. Electrost.* **2004**, *62 (1)*, 63–72. DOI: https://doi.org/10.1016/j.elstat.2004.05.001

[29] B. Cordero, V. Gómez, A. E. Platero-Prats, M. Revés, J. Echeverría, E. Cremades, F. Barragán, S. Alvarez, *Dalton Trans.* **2008**, *21*, 2832–2838. DOI: https://doi.org/10.1039/b801115j